C2SMART
CONNECTED CITIES WITH SMART TRANSPORTATION
A USDOT University Transportation Center

New York University
Rutgers University
University of Washington
The University of Texas at El Paso
City College of New York

Modeling and Optimizing Ridesourcing Services in Connected and Automated Cities

November 2021

TECHNICAL REPORT STANDARD TITLE PAGE

1. Report No.	2.Government Accession No.	3. Recipient's Catalog No.
4. Title and Subtitle Modeling and Optimizing Ride-sourcing Services in Connected and Automated Cities		5. Report Date November 2021 6. Performing Organization Code
7. Author(s) Xuegang (Jeff) Ban, 0000-0003-3605-971X; Yinhai Wang, 0000-0002-4180-5628; Don Mackenzie, 0000-0002-0344-2344; Rong Fan, 0000-0002-6558-8306		8. Performing Organization Report No.
9. Performing Organization Name and Address Connected Cities for Smart Mobility towards Accessible and Resilient Transportation Center (C2SMART), 6 Metrotech Center, 4th Floor, NYU Tandon School of Engineering, Brooklyn, NY, 11201, United States		10. Work Unit No. 11. Contract or Grant No. 69A3551747119
12. Sponsoring Agency Name and Address Office of the Assistant Secretary for Research and Technology University Transportation Centers Program U.S. Department of Transportation Washington, DC 20590		13. Type of Report and Period Covered Final Report 2020/3/1-2021/9/30 14. Sponsoring Agency Code

15. Supplementary Notes

16. Abstract

This project proposes a modeling framework to integrate ride-sourcing services and connected/automated vehicles with transit to serve different users in an urban area. Multiple travel modes are considered for morning commute: single ride and shared ride in ride-sourcing, and integrated ride-sourcing (either single ride or shared ride) and transit. Simulation testing and validation will be conducted on a multi-modal network in the Seattle area.

17. Key Words	18. Distribution Statement
Autonomous vehicles; Commuting; Connected vehicles; Multimodal transportation; Optimization; Public transit; Ridesourcing; Simulation; Urban areas; Validation	Public Access

19. Security Classif (of this report)	20. Security Classif. (of this page)	21. No of Pages	22. Price
Unclassified	Unclassified	40	

Form DOT F 1700.7 (8-69)

Modeling and Optimizing Ridesourcing Services in Connected and Automated Cities

PI: Xuegang (Jeff) Ban
University of Washington
ORC-ID: 0000-0003-3605-971X

Co PI: Yinhai Wang
University of Washington
ORC-ID: 0000-0002-4180-5628

Rong Fan
University of Washington
ORC-ID: 0000-0002-6558-8306

Co PI: Don Mackenzie
University of Washington
ORC-ID: 0000-0002-0344-2344

Disclaimer

The contents of this report reflect the views of the authors, who are responsible for the facts and the accuracy of the information presented herein. This document is disseminated in the interest of information exchange. The report is funded, partially or entirely, by a grant from the U.S. Department of Transportation's University Transportation Centers Program. However, the U.S. Government assumes no liability for the contents or use thereof.

Acknowledgements

The project team is grateful for financial and administrative support from the C2SMART UTC. The team also appreciates the discussions with and support from Seattle Department of Transportation (SDOT)

Executive Summary

Commute congestion increases alongside increases in the prosperity of cities. With the rapid development of ridesourcing services and advances in connected and automated vehicles (CAV), researchers are seeking innovative approaches to alleviate commute congestion by integrating CAV-based ridesourcing and transit services. In this research, we developed a general equilibrium modeling framework for an integrated, multimodal CAV ridesourcing and transit system to study customers' mode choices and resulting congestion patterns. The proposed framework and the modeling results are expected to provide useful insights to ridesourcing companies, transit agencies, and city managers about integrating ridesourcing and transit to better solve issues related to urban commuting.

Our model captures the choices and interactions of the three major elements in the morning commuting problem:

1. The first is a ridesourcing company that owns all CAVs and provides single-ride or shared-ride services; these services can either serve a whole trip or serve the first mile and then integrate with the transit system. The ridesourcing company's objective is to maximize its overall profit.
2. The second comprises commuters (or customers) who can choose among different mobility modes based on their preferences/utilities. The commuter's utility function captures the major factors that affect the mode choice decisions of customers, including the fixed, time/distance-based fare for ridesourcing or transit trips, the time/distance-based disutility, and disutilities due to waiting, transferring from ridesourcing to transit, and matching with another commuter if the ride is shared. Customers choose the mode from which they predict they will experience the highest utility.
3. The third comprises the route choices of all CAVs, which follow Wardrop's first principle. The total vehicle miles traveled (VMT(and vehicle hours traveled (VHT) of all vehicles are calculated for different customer mode choices.

Each element has its own decision variables, objective function, and constraints. The decision models of the three elements are connected by exogenous variables, collectively formatting a general equilibrium problem. We derived the Karush-Kuhn-Tucker (KKT) conditions of the three models and reformulated the models into a mixed domplementarity problem, which can be solved by using the PATH solver in the General Algebraic Modeling System (GAMS).

The results showed that the demand for shared rides and transit is affected by the relative costs of different types of travel modes in the integrated system. While transit use generally reduces congestion, ridesharing alone may still generate greater congestion than solo driving because of deadhead miles.

Our model can help systematically investigate the mode choices of customers and measure the resulting congestion effects in a multimodal network, which may provide valuable insights to transportation planners, transit agencies, and ridesourcing companies. Further research is recommended to include other ridesourcing modes such as on-demand transit (i.e., micro-transit) and bikeshare services.

Table of Contents

List of Figures

List of Tables

1. Introduction

Enabled by increasing smartphone use, ridesourcing companies (e.g., Uber/Lyft/Didi) have made remarkable progress in serving urban travel demand through real-time matching of drivers and customers (Ke et al., 2019). In New York City, for example, ridesourcing served 4.2 billion trips in 2018, up from about 2 billion trips in 2016, which was also more than eight times the number of trips served by taxis in 2018 (Schaller, 2018). Platforms that offer "ridesourcing," also referred to as "e-hailing" or "ride-hailing" (Shaheen et al., 2015), such as Uber Pool, may also provide shared-ride (i.e., "ridesplitting") services for customers from different (mostly two) locations.

Meanwhile, rapidly evolving vehicle automation technology has the potential to reduce vehicle ownership and increase the need for ridesourcing services, which will provoke another revolution in urban mobility (Meyhofer, 2018). However, rapid growth of ridesourcing may also lead to more car travel and urban congestion (Ban et al., 2019; Schaller, 2017). To mitigate congestion impacts, ridesourcing—especially when connected and automated vehicles (CAVs) are widely deployed—must be properly integrated with public transit to provide more accessible and efficient modes to all travelers in urban areas.

In this project, we aimed to develop a modeling framework for integrating ridesourcing with transit that is not only mathematically rigorous but also captures the key behaviors and intersections of the major elements. To illustrate our approach, we focused on the morning commute, one of the most important daily trips, which also experiences the most congestion. We modeled fixed-route mass transit, such as light rail or subway operating on a fixed schedule. There are three major elements when ridesourcing and transit services are integrated with CAVs. The first comprises customers who choose mobility services on the basis of their values of time and other personal/social characteristics. The second is a ridesourcing platform that provides both single-ride and shared-ride services, and that usually serves customers and dispatches vehicles (CAVs) to maximize its profit. The third comprises the route choices of CAVs, which affect overall network congestion. Clearly, the three elements have distinct objectives; however, they interact with each other on the multimodal transportation network of an urban area, resulting in the usage patterns of each travel mode and overall network congestion. Therefore, understanding and modeling the behaviors and the interactions of these three elements are crucial for better integrating ridesourcing and transit and for evaluating their collective effects on the urban transportation system.

We proposed a general equilibrium model for a multimodal network that captures the behaviors and interactions of the three elements and that is sensitive to customers' values of time and system congestion effects. Our model significantly extends the model by Ban et al. (2019) to encompass shared rides and transit within the CAV environment. The main tasks of this project were as follows:

1. Develop methods to model the behaviors of the three major elements (customers, providers, CAV route choices) on a multimodal network, including the development of an extended network structure.
2. Formulate a general equilibrium model that includes single rides, shared rides, and transit services with CAVs.
3. Conduct a formal analysis of the model, including the existence and uniqueness of its solution, and solution methods.
4. Evaluate the network effects resulting from different CAV dispatch strategies, customers' different values of time, and different transit usage rates.

This will provide useful insights for the development of policies to manage ridesourcing and to better integrate it with transit services.

2. Literature Review

On-demand transit systems, i.e., the integration of demand responsive services and transit, have been studied long before the era of ridesourcing. In this section, we cover a literature review of on-demand transit systems before the era of ridesourcing and also the integration of ridesourcing with transit, which has been a trending research topic in recent years.

2.1 Demand Responsive Transportation Systems and Paratransit

As early as the 1970s, the U.S. Department of Transportation was researching ''demand responsive'' transportation systems and ''paratransit'' (Orski, 1976). The purpose of on-demand systems is to provide transit services to people who live far away from transit stations, elderly people, or handicapped people to improve the equity of transit services and increase transit usage.

One of the outcomes of this research has been the integration of Dial-a-Ride and transit. Stein (1978) analytically investigated a Dial-a-Ride transportation system in which the first/last mile of public transit were served by Dial-a-Ride. The static case and the dynamic case were both studied under the assumption of uniformly distributed demand. The proposed transportation system design was computationally efficient and easy to implement. Malucelli et al. (1999) designed a demand adaptive system in which buses could pick up passengers at either compulsory stops or optional stops. In comparison with demand responsive systems such as Dial-a-Ride, the demand adaptive system still operated within a conventional line transportation framework and was considered to be more cost-effective.

2.2 The Integration of Ridesourcing with Transit

The wide deployment of ridesourcing services has inspired research into the integration of ridesourcing and transit. Feigon and Murphy (2016) examined the relationship between public transportation and ridesourcing. With survey data collected from transportation officials and shared mobility users, the authors analyzed capacity, demand, and the comparative travel times of ridesourcing and transit. An assessment of the integration of ridesourcing with transit was presented, and the complexities of current related business models were evaluated. The numerical results indicated that an increase in usage of ridesourcing was associated with higher transit usage, lower private car ownership, and

reduced transit operation costs. The authors concluded that tidesourcing, especially ridesplitting (i.e., shared rides in ridesourcing services), can complement public transit and enhance urban mobility. On the basis of these findings, public transportation agencies were encouraged to engage with ridesourcing platforms. According to the interviews and survey, public transit agencies and ridesourcing platforms have agreed on such collaborations, and some of them have already launched related projects.

Chen et al. (2017) explored design options for integrating e-hailing services into public transportation networks. Relative spatial positioning (RSP) of e-haling services was designed, which disaggregates e-hailing services in space and matches them with transit. Two types of RSPs were analyzed and compared: a zone-based design that assigned a set of e-haling vehicles to serve first/last mile within a relatively small zone surrounding a transit stop; and a line-based design that operated e-hailing vehicles along a fixed-route transit line to serve passengers who needed a ride between their origin/destination and the closest transit stop. Their study contributed to the research field by proposing a unifying analysis framework based on the continuous approximation approach and offering the first comparative study of RSP design. Their analytical and simulation results suggested that line-based services can achieve higher efficiency because the e-haling vehicles in the zone-based design incurred more deadhead miles.

Ma et al. (2019) proposed a ridesharing scheme with integrated transit in which ridesourcing served either the whole trip or the first/last mile of a transit route. Their objective was to optimize vehicle dispatch and idle vehicle relocation for an integrated, multimodal transit-rideshare system. The model had three modes: ridesharing only, rideshare-transit-rideshare, and rideshare-transit-walk (and vice versa). Dynamic queueing-theoretic vehicle dispatch and idle vehicle relocation algorithms were customized to solve the model. The numerical experiments indicated that the transit-rideshare system outperformed the rideshare-only system by a 32 percent reduction in user travel time and a 64 percent reduction in vehicle travel time. In comparospm with the rideshare-only system, the transit-ridesharing system also reduced operational costs and customer waiting times, and it achieved better performance in regions where passenger demand was heterogeneous.

Pinto et al. (2019) proposed a bi-level mathematical programming formulation for joint transit network redesign and mobility service fleet size determination. The authors tested their model framework by using real-world travel demand data. The numerical results indicated that the integrated system

reduced average customer waiting time in comparison with the transit-only system. The integration in their study was meant to replace inefficient transit routes/patterns with shared connected autonomous mobility services, while on-demand first/last mile for transit was not considered. In addition, their model had only one objective function to minimize the disutility of customers, with no ridesourcing platform profit maximization or congestion consideration.

In addition to studies on the operation of integrated transit and ridesourcing systems, researchers have also investigated user experiences and passenger preferences. Yan et al. (2019) evaluated travelers' responses to the integrated transit pilot MTransit. MTtransit was a pilot of on-demand transit services at the north campus of the University of Michigan, where twelve fixed bus routes were replaced with four fixed, high-frequency bus routes in the central high-volume corridors, together with on-demand shared shuttle services in the outer areas. Both revealed preference and stated preference data were collected from students, faculty, and staff from the campus. The study showed that ridesourcing could complement transit by serving the first/last mile and/or replacing low usage transit routes, leading to reduced passenger waiting times and lower transit operational costs.

While these other studies revealed how an integrated transit system may be designed and optimized, it is also important to evaluate how actual pilot programs bring changes to a transit system. Terry and Bachmann (2020) evaluated the types of trips passengers took though a transit-integrated ridesourcing pilot program and compared them with transit and walking alternatives. The results suggested that most rides with the pilot program saved time in comparison to the alternative modes. Ridesourcing showed the potential to complement or supplement the existing transit services. When ridesourcing only served the first/last miles, passengers chose ridesourcing over walking and were more likely to take transit; thus transit usage increased. However, there were cases (18 percent trips) when ridesourcing trips were designed alongside transit, which often led to a decrease in transit usage. There was a great chance (65 percent of the trips) that ridesourcing would not deliver passengers to their closest transit stop.

2.3 More Related Studies

Di and Ban (2019) proposed a theoretical framework for generic traffic network equilibria to model a multimodal network that consisted of solo driving, ridesharing, and e-hailing service. It was challenging to fit ridesharing in an equilibrium model. Therefore, the authors proposed an extended network

representation, including two layers: a vehicular flow layer and a person flow layer. It was critical to split the network because the vehicular flow was different from the person flow for the ridesharing mode. In this work, we formulated the ridesharing mode on the basis of ridesharing pairs instead of origin-destination pairs. We also designed two layers of network for ridesourcing (single ride and shared ride) and transit, respectively. In this way, the different properties of the transit network and ridesourcing network, such as capacity and routes, could be captured.

Ban et al. (2019) proposed a general equilibrium model that consisted of optimization for three main elements: profit optimization of service providers, including traditional taxi and e-hailing services; utility maximization for customers who could choose among solo driving, taxi, or e-hailing; and network congestion minimization, following Wardrop's principle so that vehicles would always choose the route with the minimum travel time (Wardrop and Whitehead, 1952). Numerical experiments showed customer choices under different values of time or different prices for the mobility services and the resulting congestion patterns of the network. Their study provided insights to help transportation planning agencies leverage the mode split of a multimodal network to reduce congestion. The deadhead miles of either taxi or e-haling services were found to generally exacerbate network congestion, but when the demand pattern had a high level of symmetry, the model could optimize the route choice to reduce deadhead miles. Our proposed scheme to optimize ridesourcing services significantly extends the model by Ban et al. (2019) to encompass shared rides and transit within the CAV environment.

Most studies have focused on integrated ridesourcing and transit without considering other possible modes that customers may choose, e.g., ridesourcing services alone (single rides or shared rides) for an entire trip. Pinto et al. (2019) did consider multimodal services but platform profit maximization or congestion effects were not considered. Therefore, our project will provide new perspectives on the integrated transit system.

3. Methodologies

3.1 Problem Statement

Figure 1 (a) illustrates the morning commute scenario. Four types of modes, $m \in \{1,2,3,4\}$, serve commuters from their residential areas to their worksites: i) single rides from the origin to the destination, m=1; ii) shared rides that take passengers from two separate, nearby locations from origin to destination, m=2; iii) single rides as the first mile and then a transfer to transit, m=3; and iv) shared rides that take passengers from two separate locations as the first mile and then a transfer to transit, m=4. Single-ride services and shared-ride services are operated by the same ridesourcing platform. We refer to the four types of modes as taxi (m=1), ridesharing (m=2), Ttransit (taxi and transit, m=3), RStransit (ridesharing and transit, m=4); see Figure 1 (b). A customer chooses a particular mode on the basis of an individual value of time and other characteristics.

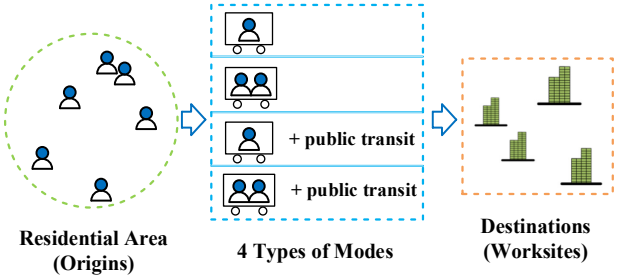

(a) Morning commute scenario

	Single ride	Shared ride
Ridesourcing mode	Taxi, m= 1	Ridesharing, m=2
Integrated mode	Ttransit, m=3	RStransit, m=4

(b) Four types of modes

Figure 1: Integrated multimodal network

Here we did not consider the mode in which a commuter would own a CAV and drive alone to the worksite (i.e., the "solo driving" mode as defined in Ban et al. (2019)) in order to better investigate the interaction between CAV ridesourcing and transit. The transit services considered were mass transit with fixed routes/schedules (i.e., on-demand transit services were not considered), such as light rail, subway, or bus rapid transit (BRT); those usually operate on a separate right-of-way and thus have little or no interaction with vehicular traffic congestion. Additionally, for the current study, we only considered shared rides in which a CAV would pick up customers from a maximum of two separate nearby locations. This was consistent with the ridesplitting services of most ridesourcing platforms (e.g., Uber Pool), and research has suggested that in practice, more than 90 percent of shared rides include two pick-up locations (Li et al., 2019). The proposed modeling framework may be further extended to include solo driving, on-demand transit, and street bus services, which we have left for future research.

3.2 General Equilibrium Overview

We proposed a general equilibrium model with three modules (Figure 2). In the ridesourcing choice module, we maximized the revenue of the provider. The endogenous variable was the CAV dispatch (i.e., vehicle supply), while customer demand and route choice were exogenous variables. In the customer choice module, we minimized the disutility of customers. The decision variables were the demand of each mode, with vehicle supply and route choices as the exogeneous variables. The network congestion module captured the flow interaction and congestion effects due to the choices and interaction of customers and service providers. We modeled the behavior of vehicles' route choices according to Wardrop's first principle, i.e., CAVs always chose the route with the minimum travel time. The route choice was the decision variable, while demand and vehicle supply were exogenous variables. The three modules combined to form a general equilibrium model.

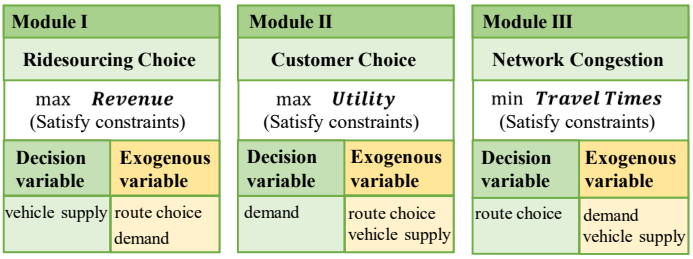

Figure 2 A summary of the general equilibrium model

3.3 Extended Network Structure

We constructed an extended network of two layers to model the integrated multimodal network, similar to the method used by Di and Ban (2019) but more concise. Figure 3 shows the extended structure for a small network. Figure 3 (b) is the ridesourcing layer, where node 5 is the vehicle destination for ridesourcing (m=1,2), and transit station node 4 is the vehicle destination for the integrated modes (m=3,4). For the transit layer (Figure 3 (a)), we defined transit nodes 6 and 7, where node 6 had the same location as node 4 in the ridesourcing layer, and node 7 had the same location as node 5 (Figure 3 (c)). Vehicle flow was based on the ridesourcing layer, while passenger flow was based on both layers. Recall that our model assumed that transit would run on separate right-of-way and therefore would not interact with congestion in the ridesourcing layer. To simplify the discussion, in this study, we only considered that CAV ridesourcing would serve the first mile of transit and thus assumed that customers' destinations would coincide with transit stations. A similar method could be applied to model a scenario in which CAV ridesourcing served the last mile of transit when customers' destinations were different from transit stations. The proposed model can also deal with multiple transit stations at the origins

and/or at the destinations, although only one such station is shown (at the origins or at the destinations) in Figure 3 for illustration purposes.

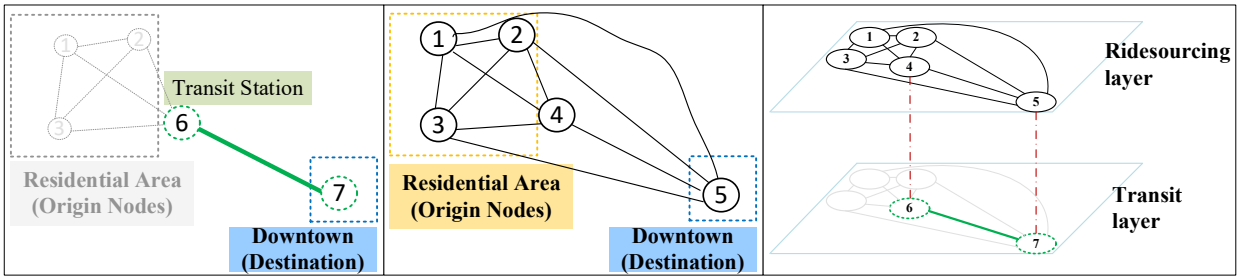

(a) Transit layer (b) Ridesourcing layer (c) Two-layer network

Figure 3 Extended network structure of the small network

4. Model Formulation

We define the following sets in our model: $m \in \{1,2,3,4\}$, four types of modes, described in section 2.1; N, the set of nodes; O, the set of origins, where vehicles pick up passengers; D^v, the set of destinations of ridesourcing vehicles, where vehicles drop off all passengers and then head to the next pick-up location; D^c, the set of destinations of customers, which are the worksites; $K \in O \times D^c$, the set of origin-destination (OD) pairs for customers; and T, the set of transit stations, where customers of mode 3 or 4 transfer to transit. In the model formulation, O_k denotes the origin of an OD pair k, D_k^v denotes the vehicle destination of the OD pair k, D_k^c denotes the customer destination of the OD pair k, T_k denotes the transit station of the OD pair k for mode 3 or 4. That is, vehicles and customers have different destinations for the integrated transit modes (m=3,4) but have the same destination if the whole trip is served by the ridesourcing modes (m=1,2). Here we define a mapping set $MAP \coloneqq \{(m, D^v, D^c), k \in K | (1, D_k^c, D_k^c),\ (2, , D_k^c, D_k^c),\ (3, D_k^v, D_k^c),\ (4, D_k^v, D_k^c)\}$ to connect the sets of customer destinations and CAV destinations of each mode. To illustrate these sets using the network in Figure 3, we have $N \coloneqq \{1,2,3,4,5\}$, $O \coloneqq \{1,2,3\}$, $D^v \coloneqq \{4,5\}$, $D^c \coloneqq \{5\}$, $T_k \coloneqq \{6\}$, $MAP \coloneqq \{(m, D^v, D^c) | (1,5,5),\ (2,5,5),\ (3,4,5),\ (4,4,5)\}$.

4.1 Ridesourcing Choice Module (*Module I*)

The revenue of each shared-ride vehicle consists of a fixed fare, time-based fare, and distance-based fare for each passenger. The fixed fares $F_{O_k}^m$ and $F_{O_{k'}}^m$ for two shared-ride passengers with OD pairs k and k' are based on the locations of the origin nodes, O_k and $O_{k'}$. Notice that although the vehicle takes detours to pick up passengers, the fare that passengers need to pay is based on the distance between their origins and the destination. Thus the time- and distance-based fares are formulated as $\alpha_1^m\left(t_{O_kD_k} + t_{O_{k'}D_k}\right)$ and $\alpha_2^m\left(d_{O_kD_k} + d_{O_{k'}D_k}\right)$

where α_1^m is the time-based fare rate and α_2^m is the distance-based fare rate. Notice here that for simplicity, we assume the two groups of passengers on a shared ride go to the same destination (i.e., the same transit stop or the same downtown worksite). The modeling method proposed here can be properly revised to incorporate the case in which the two destinations are separate and close to each other.

The cost of each shared-ride vehicle also includes time- and distance-based costs of the actual route taken, represented by $\beta_1^m\left(t_{jO_k} + t_{O_kO_{k'}} + t_{O_{k'}D_k}\right)$ and $\beta_2^m\left(d_{jO_k} + d_{O_kO_{k'}} + d_{O_{k'}D_k}\right)$

where β_1^m is the time-based cost rate and β_2^m is the distance-based cost rate. Since we specifically model CAVs, the time-based cost will be lower than it is for traditional taxis. However, if a vehicle takes longer than usual to finish a trip, it indicates less efficiency and lower customer satisfaction, which

create extra cost to the platform. In summary, the profit function of a shared-ride vehicle that drops off the previous passenger(s) at j and then picks up passengers first at O_k and then at $O_{k'}$ can be formulated as follows:

$$R^m_{jkk'} = F^m_{O_k} + F^m_{O_{k'}} + \underbrace{\alpha^m_1\left(t_{O_kD_k} + t_{O_{k'}D_k}\right)}_{\substack{time\ based\\ revenue}} + \underbrace{\alpha^m_2\left(d_{O_kD_k} + d_{O_{k'}D_k}\right)}_{\substack{distance\ based\\ revenue}} - \underbrace{\beta^m_1\left(t_{jO_k} + t_{O_kO_{k'}} + t_{O_{k'}D_k}\right)}_{travel\ time\ based\ cost} - \underbrace{\beta^m_2\left(d_{jO_k} + d_{O_kO_{k'}} + d_{O_{k'}D_k}\right)}_{travel\ distance\ based\ cost} \quad \forall m = 2,4$$

Similarly, the profit of a single-ride vehicle that drops off the previous passenger(s) at j and then picks up passengers at O_k and drop off passengers at destination D_k can be formulated as follows:

$$R^m_{jk} = F^m_{O_k} + \underbrace{\alpha^m_1 t_{O_kD_k}}_{\substack{time\ based\\ revenue}} + \underbrace{\alpha^m_2 d_{O_kD_k}}_{\substack{distance\ based\\ revenue}} - \underbrace{\beta^m_1\left(t_{jO_k} + t_{O_kD_k}\right)}_{travel\ time\ based\ cost} - \underbrace{\beta^m_2\left(d_{jO_k} + d_{O_kD_k}\right)}_{travel\ distance\ based\ cost} \quad \forall m = 1,3$$

For $m = 1$ or 2, commuters take single rides or shared rides to their actual destinations (e.g., in Figure 3, the drop-off location is node j=5); for $m = 2$ or 4, commuters take single rides or shared rides to the transit stations (not their actual destinations), e.g., in Figure 3, the drop-off location is node j=4 (the same as node 6 in the transit layer). This needs to be properly modeled using the *MAP* set.

The decision variables of the ridesourcing choice module are $z^m_{jkk'}$ (where $O_k, O_{k'} \in O$) for shared-ride vehicles and z^m_{jk} (where $O_k \in O$) for single-ride vehicles. $z^m_{jkk'}$ denotes the number of shared-ride vehicles currently at destination j that will next pick up customers first at O_k and then at $O_{k'}$. z^m_{jk} denotes the number of single-ride vehicles currently at destination j that will next pick up customers at O_k. Although there are four types of modes, the ridesourcing platform provides only two types of services, either single rides or shared rides. Here we assume that for the same service, the platform has the same price strategies for first-mile trips and whole trips. The objective function of *Module I* is to maximize the total profit from single-ride and shared-ride services:

$$\max_{z^m_{jk}\geq 0, z^m_{jkk'}\geq 0, q^m_{kk'}, b^m_{kk'}} \underbrace{\sum_{m=1,3} R^m_{jk} z^m_{jk}}_{single\ ride} + \underbrace{\sum_{m=2,4}\left(R^m_{jkk'} z^m_{jkk'} - \omega^m \cdot \left|q^m_{kk'}\right| - \omega^m \cdot \left|b^m_{kk'}\right|\right)}_{shared\ ride}$$

subject to the following constraints:

Constraints for single rides, $m = 1,3$:

$\sum_{j\in D} z^m_{jk} \geq Q^m_k \quad \forall\, k \in K$ *vehicle supply satisfies customer demand*

$\sum_{k\in K} z_{jk}^{m} = \sum_{k':\ j=D_k} Q_{k'}^{m} \quad \forall\, j \in D$ *vacant single-ride CAVs are available again to serve the next trip*

Constraints for shared rides, $m = 2,4$:

$\sum_{j\in D} z_{jkk'}^{m} - Q_{k,kk'}^{m} = b_{kk'}^{m}, \ \forall k \in K$ *shared vehicles pick up two customers in each trip*

$\sum_{j\in D} z_{jkk'}^{m} - Q_{k',kk'}^{m} = q_{kk'}^{m} \quad \forall k \in K$ *shared vehicles pick up two customers in each trip*

$\sum_{k,k'\in K} z_{jkk'}^{m} = \sum_{k\in K}\sum_{k':\ j=D_{k'}} Q_{k',kk'}^{m} \quad \forall j \in D$ *vacant shared-ride CAVs are avaible again*

Constraint for the total number of vehicles:

$$\underbrace{\sum_{m=1,3}\left(\sum_{k\in K}\sum_{j\in D} z_{jk}^{m} t_{jO_k} + \sum_{k\in K} Q_{k}^{m} t_{O_kD_k}\right)}_{number\ of\ vehicles\ for\ sigle\ ride} + \underbrace{\sum_{m=2,4}\left(\sum_{k,k'\in K}\sum_{j\in D} z_{jkk'}^{m} t_{jO_k} + \sum_{k,k'\in K} Q_{k,kk'}^{m} t_{O_kO_{k'}} + \sum_{k,k'\in K} Q_{k',kk'}^{m} t_{O_{k'}D_{k'}}\right)}_{number\ of\ vehicles\ for\ shared\ ride} \le N$$

Here Q_k^m is the demand of mode *m* for OD pair *k*. $Q_{kk'}^m$ and $Q_{k'k}^m$ are the demand of the fist pick-ups and second pick-ups of the shared ride services (m=2,4). As illustrated in Figure 2, customer demand variables are exogenous to *Module I*.

$q_{kk'}^m$ and $b_{kk'}^m$ are defined to capture the mismatch of the first and second pick-ups of shared rides. A mismatch occurs either when there are not enough shared-ride vehicles to pick up two passengers from two different origin nodes ($b_{kk'}^m < 0$ or $q_{kk'}^m < 0$) or when there are more shared-ride vehicles than the number of customers who need to be picked up ($b_{kk'}^m > 0$ or $q_{kk'}^m > 0$). Taking ridesharing (m=2) as an example, $b_{kk'}^2 = 0$ indicates that the number of ridesharing vehicles equals the number of customers who are picked up first; $q_{kk'}^2 = 0$ indicates that the number of ridesharing vehicles equals the number of customers who are picked up second. Thus, there is no mismatch when both $q_{kk'}^2$ and $b_{kk'}^2$ equals 0. Similar analysis applies to RStransit. We define ω^m as the rate of penalty, with a higher value indicating a greater cost per mismatch. Constraints for *Module I* ensure the following: i) the number of vehicles dropping off customers at destination *j* is equal to the number of vehicles departing from *j*; ii) each customer request is served ; iii) shared-ride vehicles can pick up at most only two passengers from up to two different origins, and penalties will be imposed if they pick up passengers from only one location; iv) the number of vehicles in operation is no larger than the total number of vehicles operated by the platform.

4.2 Customer Choice Module (*Module II*)

Customers can choose to take ridesourcing to a transit station or directly to worksites. Therefore, the customer flow is present on both the ridesourcing layer and the transit layer. When the disutility of the

shared-ride customers is calculated, either for the first mile or for the whole trip, there is a trade-off between precisely capturing the behavior of the customers and the feasibility of the model. For shared-ride trips, the first customer tends to have a longer ride time while the second customer tends to have a longer waiting time. But if the shared-ride trips benefit the first customer more than the second customer, it will be hard for the model to find a second customer so that the model is feasible. Therefore, we simplify travel/waiting time-based disutility so that two customers in the same shared-ride trip expect the same (worst-case) disutility caused by the detour. The disutility of a shared-ride customer that is picked up first can be formulated as follows,

$$V_{kk'}^m = \underbrace{F_{O_k}^m}_{\substack{fixed\\ fare}} + \underbrace{\alpha_1^m t_{O_k D_k}}_{\substack{travel\ time\\ based\ fare}} + \underbrace{\alpha_2^m d_{O_k D_k}}_{\substack{distance\ based\\ fare}} + \underbrace{\gamma_1^m (t_{O_k O_{k'}} + t_{O_k D_k})}_{\substack{travel\ time\\ based\ disutility}} + \underbrace{\gamma_2^m t_{O_k O_{k'}} + w_{kk'}^m}_{\substack{disutility\ due\\ to\ waiting}} + \underbrace{\gamma_3^m \lambda_{kk'}^m}_{\substack{disutility\ due\\ to\ matching}} + Tr_k^m \quad \forall m = 2,4$$

where O_k is the first pick-up location and $O_{k'}$ is the second pick-up location. We have disutility due to the fare of the shared rides. $F_{O_k}^m$ is the location-based fixed fare. The time-based fare $\alpha_1^m t_{O_k D_k}$ and the distance-based fare $\alpha_2^m d_{O_k D_k}$ depend only on the OD pair $O_k \to D_k$, which is reasonable because the additional disutility of shared rides is already considered in other terms. γ_1^m is the disutility rate for travel time. The travel time disutility depends on the travel time of OD pair $O_k \to D_k$ and the travel time of detour $O_k \to O_{k'}$. We define γ_2^m as the waiting time disutility rate and $w_{kk'}^m$ as the waiting time disutility from the previous drop-off location to the first pick-up location. Therefore the summation of $\gamma_2^m t_{O_k O_{k'}}$ and $w_{kk'}^m$ captures the worst-case waiting time from the vehicle's previous drop-off location j to the second shared-ride customer. The matching of the two customers in a shared ride is also regarded as the cost of the platform, which is modelled as the Lagrange multiplier of the shared ride demand constraints in *Module I*. This is denoted as $\gamma_3^m \lambda_{kk'}^m$, where γ_3^m is the rate of matching cost and $\lambda_{kk'}^m$ is the multiplier. See Ban et al. (2019) for more discussions of why this multiplier could be regarded as (proportional to) the matching cost. The disutility of the second picked-up customer, $V_{k'k}^m$, can be derived similarly, which is omitted here.

We assume high capacity for the transit route $T_k \to D_k$, so the travel time and distance are constant for the transit route. Consequently, travel time and travel distance can be represented by the same parameter, $t_{T_k D_k} \cdot const = d_{T_k D_k}$. The disutility of taking transit consists of the time/distance-based transit fare $\alpha_3^m d_{T_k D_k}$, time/distance-based disutility $\gamma_4^m d_{T_k D_k}$, and the transfer cost γ_5^m. When $m = 1,2$, ridesourcing vehicles serve the whole trip, so $Tr_k^m = 0$. Therefore, the disutility of transit is

$$Tr_k^m = 0 \quad \forall m = 1,2$$

$$Tr_k^m = \underbrace{\alpha_3^m d_{T_k D_k}}_{\substack{travel\ distance\\ based\ fare}} + \underbrace{\gamma_4^m d_{T_k D_k}}_{\substack{travel\ distance\\ based\ disutility}} + \underbrace{\gamma_{T_k D_k}^m}_{\substack{disutility\ of\\ transfer}} \quad \forall m = 3,4$$

As with shared rides, the disutility of a customer of a single-ride trip can be formulated as follows,

$$V_k^m = \underbrace{F_{O_k}^m}_{fixed\ fare} + \underbrace{\alpha_1^m t_{O_k D_k}}_{\substack{travel\ time \\ based\ fare}} + \underbrace{\alpha_2^m d_{O_k D_k}}_{\substack{distance\ based \\ fare}} + \underbrace{\gamma_1^m t_{O_k D_k}}_{\substack{travel\ time \\ based\ disutility}} + \underbrace{w_k^m}_{\substack{disutility\ due \\ to\ waiting}} + Tr_k^m \quad \forall m = 1,3$$

Customer waiting time is calculated as the average deadhead miles from the previous destinations to the next origin (first origin for shared ride trips); see Ban et al. (2019).

$$w_k^m = \gamma_2^m \frac{\sum_{j \in D} z_{jk}^m t_{jO_k}}{\sum_{j \in D} z_{jk}^m} \quad \forall k \in K, m = 1,3$$

$$w_{kk'}^m = \gamma_2^m \frac{\sum_{j \in D} z_{jkk'}^m t_{jO_k}}{\sum_{j \in D} z_{jkk'}^m} \quad \forall k, k' \in K, m = 2,4$$

The decision variable for *Module II* is customer demand. The customer demand for single rides is Q_k^m. The customer demand for shared rides are $Q_{kk'}^m$ and $Q_{k'k}^m$ for the first pick-up and second pick-up, respectively. The objective function minimizes the disutility of customers:

$$\min_{Q_{k'k}^m, Q_{kk'}^m, Q_k^m} \quad \sum_{m=1,3} V_k^m Q_k^m + \sum_{m=2,4} V_{kk'}^m Q_{kk'}^m + \sum_{m=2,4} V_{k'k}^m Q_{k'k}^m$$

subject to the following:

$$\sum_{m=1}^{4} Q_k^m = Q_k \quad \forall k \in K$$

$$\sum_{k' \in K} (Q_{k'k}^m + Q_{kk'}^m) = Q_k^m \quad \forall m = 2,4, k \in K$$

The constraints for *Module II* ensure the following: i) the customers requesting different types of modes sum up to the total travel demand; ii) the number of customers taking shared rides along OD pair $O_k \rightarrow D_k$ is equal to the summation of O_k as the first and second pick-up locations from all shared-ride trips. The above module minimizes the total disutility of all customers. Since V_k^m, $V_{kk'}^m$, $V_{k'k}^m$ are all exogeneous to *Module II* (as they are independent of Q_k^m, $Q_{k'k}^m$, $Q_{kk'}^m$), our formulation ensures that each customer chooses the mode with the least disutility. An analogy for this is that the shortest path search problem on a transportation network can be reformulated to a linear program to minimize the total cost of all users of the network; more discussions on this can be found in Ban et al. (2019).

4.3 Network Congestion Module (*Module III*)

Because we only consider the congestion effect of ridesourcing services, *Module III* is based on the ridesourcing layer. There are three types of network flow: i) deadhead miles, i.e., the distance CAVs travel from drop-off locations to the next pick-up locations, which apply to both single rides and shared rides; ii) detours, when CAVs are occupied by only the first group of shared-ride customers to pick up

the second group of customers, which only apply to shared rides; and iii) occupied trips, when a CAV travels from the final pick-up location to the destination, which apply to both single rides and shared rides. The following equations show how the three types of flow can be calculated.

(i) Deadhead miles: $\sum_{m=1,3} z_{jk}^{m} t_{jO_k} + \sum_{m=2,4} \sum_{k'} z_{jkk'}^{m} t_{jO_k}$

(ii) Detours: $\sum_{m=2,4} \sum_{k' \in K} Q_{kk'}^{m} t_{O_k O_{k'}}$

(iii) Ocuppied trips: $\sum_{m=1,3} Q_{k}^{m} t_{O_k D_k} + \sum_{m=2,4} \sum_{k' \in K} Q_{k'k}^{m} t_{O_k D_k}$

For each type of flow, we can formulate it as complementary conditions to ensure that the route choice follows Wardrop's principle. This approach takes after Ban et al. (2019), and details are omitted here. Now that we have the full formulation of the general equilibrium model, consisting of the three optimization problems from *Module I-III*, we can derive the KKT conditions of the three optimization problems and reformulate the general equilibrium model to a **mixed complementarity problem (MCP).** We studied and established the solution existence and uniqueness conditions to such a formulation, using methods similar to those reported by Ban et al. (2019).

5. Numerical Experiments

We solved the general equilibrium model (an MCP) by using the *PATH* solver in the General Algebraic Modeling System (GAMS). Sensitivity analysis was conducted on a small network and the Sioux Falls network. Because of space limitations, we omitted the results of the downtown Seattle network in this study. When conducting the sensitivity analysis, we first set the baseline values for all parameters; we then either unilaterally changed one parameter at a time or changed two parameters at the same time to see how customers' mode choice and the overall network congestion reacted to the changes in the parameters.

5.1 Numerical Results of the Small Network

The link properties of the small network (Figure 3) are shown in Table 1. We set the demand from nodes 1 through 3 to destination node 5 to be 40 for all three origins. Table 2 lists the baseline parameters. Essentially, parameters for all single ride vehicles were the same, either for whole trips or first-mile trips. We set the single-ride parameters for *m*=1,3 to the same values, e.g., $\alpha_1^1 = \alpha_1^3$. Similarly, we set the shared-ride parameters for mode *m*=2,4 to the same values, e.g., $\alpha_1^2 = \alpha_1^4$. The baseline parameter settings in Table 2 reflect the following relationship between the fares of different modes: single ride > shared ride > transit, while customer disutility rates follow the relation: shared-ride > single-ride. When conducting the sensitivity analysis described later in this section, we modified some of these baseline parameters.

Table 1 Parameters of the small network

Link	From	To	Length (mile)	FFT (h)	Capacity	Link	From	To	Length (mile)	FFT (h)	Capacity
1	1	2	0.4	0.02	40	11	4	2	1.8	0.06	60
2	1	3	0.5	0.025	40	12	4	3	1.8	0.06	60
3	1	4	2.1	0.07	60	13	2	5	10	0.5	100
4	2	1	0.4	0.02	40	14	3	5	11	0.55	100
5	2	3	0.6	0.03	40	15	4	5	9	0.45	120
6	2	4	1.8	0.06	50	16	5	2	10	0.5	100
7	3	1	0.5	0.025	40	17	5	3	11.5	0.55	100
8	3	2	0.6	0.03	40	18	5	4	9	0.45	120
9	3	4	1.8	0.06	50	19	6	7	9	----	----
10	4	1	2.1	0.07	60						

Table 2 Baseline parameters (small network)

Illustration of parameters	Notation (m =1,2,3,4)	Value
The fixed fare for different modes ($)	F^m	5, 2.9, 5, 2.9
Time-based fare rate ($/h)	α_1^m	4.1, 1.2, 4.1, 1.2
Distance-based fare rate ($/mile)	α_2^m	1.5, 1.7, 1.5, 1.7
Conversion factor from time to cost ($/h)	β_1^m	7, 2.6, 7, 2.6
Conversion factor from distance to cost ($/mile)	β_2^m	1, 1.1, 1, 1.1
Value of time of customers, while traveling ($/h)	γ_1^m	2, 2.7, 2, 2.7
Value of time of customers, while waiting ($/h)	γ_2^m	3, 4.2, 3, 4.2
Value of time of customers, whilce mathing in shared rides ($)	γ_3^m (m=2,4)	NA, 2.5, NA, 2.5
Travel distance-based fare rate of transit ($/h)	α_3	0.37
Conversion factor from distance to cost for transit ($/mile)	γ_4	0.22
Transfer cost of transit ($/transfer)	γ_5	1.1

5.1.1 Results of Unilaterally Changing One Parameter

Table 3 shows the results when we unilaterally changed the travel distance-based fare rate of single rides or shared rides. Under the current baseline parameter setting (Table 2), the demand for serving the whole trip using ridesourcing ($m = 1,2$) was always zero, indicating that customers preferred the integrated modes that contained both ridesourcing and transit. In comparison with Ttransit, RStransit saved more vehicle miles traveled (VMT); thus higher demand for RStransit corresponded to lower VMT. When we unilaterally increased the distance-based fare rate of single rides ($\alpha_2^1 = \alpha_2^3$), the cost of requesting Ttransit increased; thus the demand for Ttransit decreased while the demand for RStransit increased. When we unilaterally increased the distance-based fare of shared ride ($\alpha_2^2 = \alpha_2^4$), the demand for RStransit decreased while the demand for Ttransit increased. This example shows that when we increased the cost parameter related to a particular mode (which represented a certain cost/disutility of selecting the mode), customer choice of that mode decreased, and the VMT of the entire network also changed accordingly.

Table 3 Unilaterally changing α_2^1 or α_2^2

$\alpha_2^1 = \alpha_2^3$	$\alpha_2^2 = \alpha_2^4$	Taxi, m=1	Ridesharing, m=2	Ttransit, m=3	RStransit, m=4	VMT (miles)
1.45	1.73	0%	0%	100%	0%	455.90
1.47		0%	0%	70%	30%	393.14
1.53		0%	0%	33%	67%	316.00
1.85		0%	0%	21%	79%	294.69
1.93		0%	0%	0%	100%	258.00
1.52	1.19	0%	0%	23%	77%	298.36
	2.12	0%	0%	46%	54%	342.05
	2.13	0%	0%	73%	27%	399.96
	2.18	0%	0%	90%	10%	434.37
	2.20	0%	0%	100%	0%	456.00

When we unilaterally changed the waiting time cost parameter for single rides (γ_2^1), modes 1,3,4 had non-zero demand (Table 4). When we increased γ_2^1, the cost of both taxi and Ttransit increased. As a result, the demand for taxi and Ttransit decreased while the demand for RStransit increased.

Table 4 Unilaterally changing γ_2^1

$\gamma_2^1 = \gamma_2^3$	Taxi, m=1	Ridesharing, m=2	Ttransit, m=3	RStransit, m=4	VMT (miles)
1.75	33%	0%	67%	0%	1149.57
1.79	24%	0%	58%	18%	927.45
1.81	18%	0%	51%	31%	763.75
1.83	8%	0%	42%	50%	521.50
1.85	2%	0%	35%	63%	359.27

5.1.2 Results of Changing Two Parameters at the Same Time

To better show how different mode choices may impact VMT, we compared the VMT of a certain mode split scenario to the case in which all customers drove alone in a personal vehicle. Note that this mode choice was not explicitly modeled; however it could be easily computed by the user equilibrium solution. When all customers chose solo driving (no ridesourcing or transit involved), the VMT was equal to 1,266.11 vehicle miles based on the UE solution. Thus, the VMT change could be calculated as:

$$VMT\ change = (VMT\ of\ a\ particular\ scenario - 1266.11)/1266.11$$

VMT change was a better indicator of congestion level than the absolute value of VMT. When the VMT change was positive, it indicated that deadhead miles were traveled, making the congestion level higher than that of the solo driving scenario. When the VMT change was negative, it implied that many

customers chose transit or shared rides, so that the network was less congested than in the solo driving scenario.

Figure 4 shows the results when the time-based disutility rate for shared ride ($\beta_1^2 = \beta_1^4$) and the transfer cost of transit (γ_5) were changed at the same time. The demand for single rides was zero; customers chose between ridesharing and RStransit. Because the demand for ridesharing and RStransit summed up to 1, we show only the demand pattern for ridesharing (Figure 4 (a)). Figure 4 is divided into two regions; the top part is the high ridesharing demand region, and the bottom part is the high RStransit region. When γ_5 increased, the cost of taking transit increased; thus the demand for RStransit decreased and the demand for ridesharing increased. When β_1^2 increased and the transit parameter $\gamma_5 \approx 0.3$, the cost of ridesharing increased, so the demand for RStransit increased while the demand for ridesharing decreased. When customers chose between only ridesharing and RStransit, the demand pattern was mainly affected by transit parameter γ_5. When $\gamma_5 \in [0.25, 0.48]$, the ridesharing parameter also affected the demand pattern. Figure 4 (b) indicates that VMT change was consistent with the mode split pattern: VMT increased when more customers switched from RStransit to ridesharing. When γ_5 was small and most or all demand was served by RStransit, the VMT might be lower than solo driving; however, when more than about 20 percent of trips utilized ridesharing, the VMT was greater than that for solo driving.

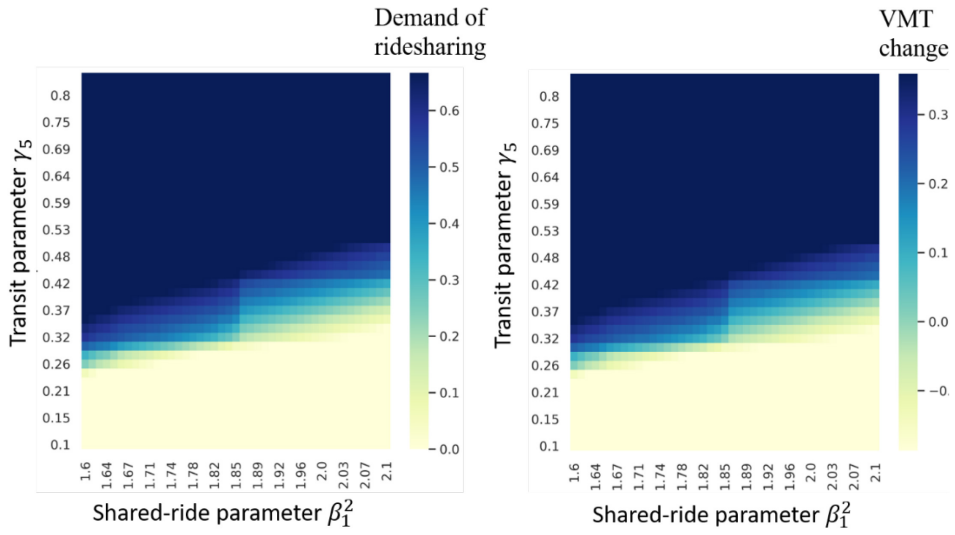

(a) Percentage of Demand of ridesharing (m=2) (b) VMT change

Figure 4 Sensitivity analysis of changing β_1^2 ($\beta_1^2 = \beta_1^4$) and γ_5

When more than two types of modes had non-zero demand, the mode split pattern could be more complex. Figure 5 shows the results of changing the distance-based fare rate of shared rides ($\alpha_2^2 = \alpha_2^4$)

and the travel distance-based cost of transit (α_3). The demand for Ttransit was always zero; customers chose among the other three modes: taxi, ridesharing, and RStransit. There were five mode split patterns, shown in Figure 5 (a)-(b). The demand and VMT change of those five mode split patterns are summarized in Table 5. Along the boundary of the different mode split patterns, the demands of different modes changed gradually, shown by the zoomed-in version of the boundaries in Figure 5 (a) and (b). Mode split pattern ① lies in the region where the transit parameter was low, $\alpha_3 < 0.1$. The disutility of taking transit was low and all customers chose RStransit. Mode split patterns ② through ⑤ roughly divide the space of transit parameter and ridesharing parameter into four quadrants. Mode split pattern ② takes place in the right bottom quadrant, where transit parameter $\alpha_3 < 0.64$ and shared-ride parameter α_2^2 is large. In comparison with pattern ①, transit cost and shared-ride cost are higher in ②. Thus 33 percent of customers switched from RStransit to taxi. Mode split pattern ③ lies next to ②, with a smaller shared-ride cost parameter. As a result of the decreased shared-ride cost, ridesharing demand increased to 67 percent, and taxi demand dropped to zero. In comparison with ②, mode split ③ also had higher transit cost parameters; thus the transit use decreased to 33 percent. Mode split ③ had lower VMT than ②, since no travelers requested taxi rides in ③. The mode split patterns ④ and ⑤ can be explained in a similar manner. From this example, we can see that the mode split in the integrated multimodal network had complex patterns. Especially in the era of CAVs, when vehicle operations will be highly coordinated, it will be even more important to systematically study customers' mode choices. The VMT changes in Figure 5 (d) are consistent with the mode split pattern seen in Figure 5 (a) – (c). The relationship between mode split and VMT change is further discussed in the following section.

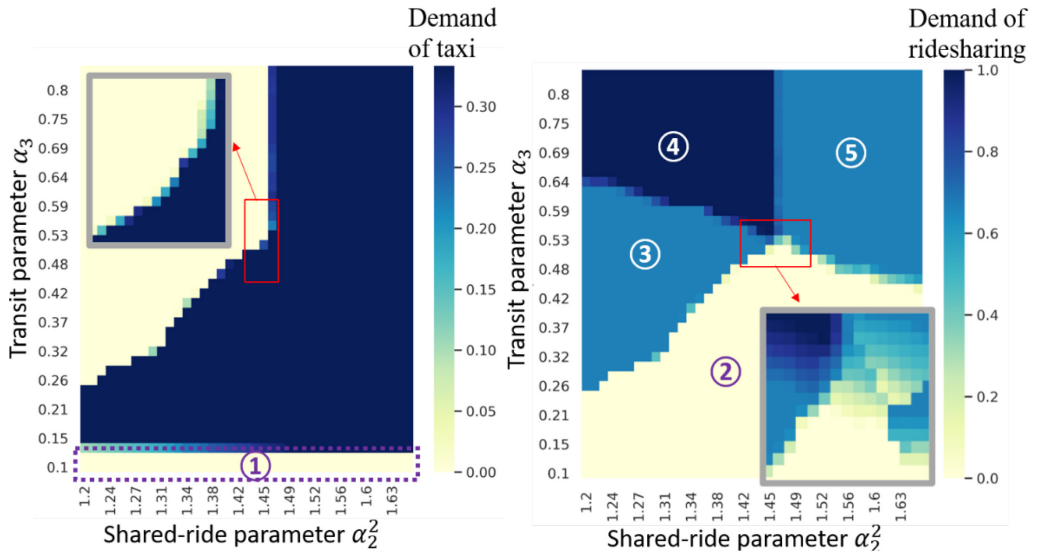

(a) Demand for taxi (m=1)

(b) Demand for ridesharing (m=2)

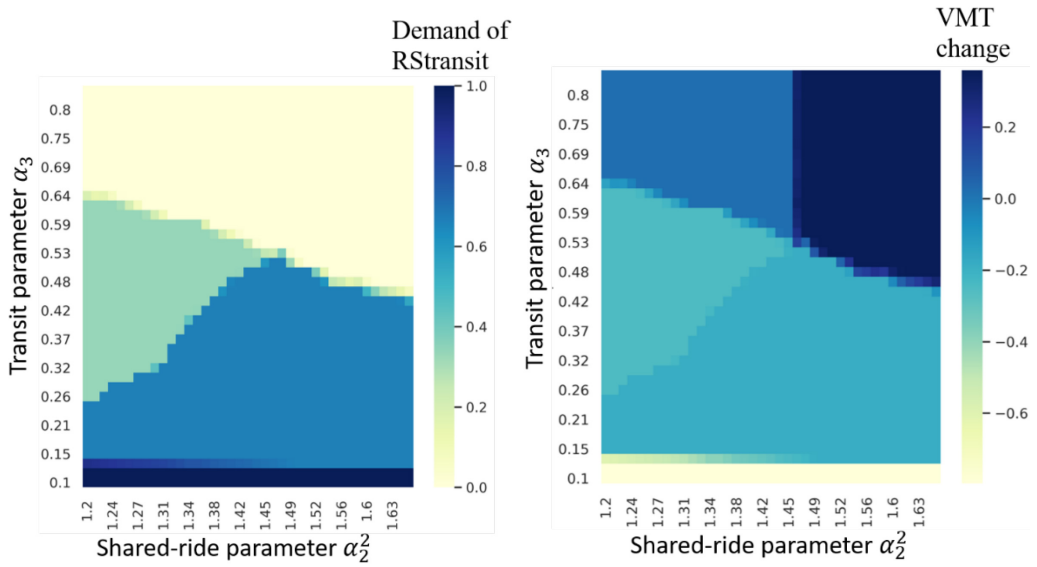

(c) Demand for RStransit (m=4)

(d) VMT change

Figure 5 Sensitivity analysis of changing α_2^2 $(\alpha_2^2 = \alpha_2^4)$ and α_3

Table 5 Summary of the mode split patterns in Figure 5

Mode split pattern	Taxi	Ridesharing	Ttransit	RStransit	VMT change
①	0%	0%	0%	100%	-80%
②	33%	0%	0%	67%	-25%
③	0%	67%	0%	33%	-30%
④	0%	100%	0%	0%	1%
⑤	33%	67%	0%	0%	33%

5.1.3 Mode Choices versus VMT Change

Figure 6 (a) through (d) shows the relationship between demand (expressed in terms of the percentage of total demand) for a particular mode $m \in \{1,2,3,4\}$ and VMT change. The plots were generated by 1) randomly changing all the model parameters (and thus the mode choices of customers and the resulting VMT of the network) and 2) showing the percentage of the demand *m* and the VMT change. For the demand percentage for a given mode, for example ridesharing (Figure 6 (b)), customers could choose among the other three modes, depending on the actual parameter combinations, resulting in different mode choices and different levels of VMT changes. Therefore, the relationship between ridesharing demand and VMT change was scattered and formed a triangular region; the variations of mode splits and VMT changes decreased as the demand percentage of ridesharing increased, which diminished when the demand percentage was 100 percent. Similar patterns were found for the other three modes. Further examination of the plots and results revealed that the upper boundary and lower boundary of each plot in Figure 6 (a) through (d) captured the cases when exactly two modes were selected. For example, in Figure 6 (d), along the upper boundary, customers chose between taxi and RStransit, while the demand for ridesharing or Ttransit was zero. Thus, the VMT change starts at the corner case of all customers choosing taxi (VMT change = 100 percent) and ends at the corner case of all customers choosing RStransit (VMT change≈ -80 percent). Along the lower boundary in Figure 6 (d), customers chose between Ttransit and RStransit while the demand for taxi or ridesharing was zero. The VMT change starts at the corner case of all customers choosing Ttransit (VMT change≈-64 percent) and ends at the corner case of all customers choosing RStransit (VMT change≈ -80 percent). The data points within the triangular region represent cases in which three or more modes were selected.

We can further show the corner cases (i.e., when customers chose only one of the four modes) in Figure 6(e). The plot shows that RStransit saved the most VMT: VMT decreased by 80 percent in comparison with solo driving when all customers chose RStransit. On the other hand, Ttransit reduced VMT by 64 percent, ridesharing had VMT similar to that ofsolo driving, and taxi caused the most congestion, with a 100 percent VMT increase because of deadhead miles.

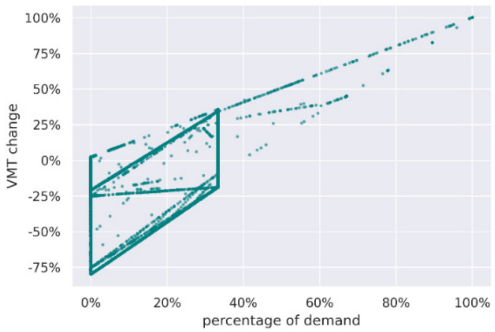

(a) Demand of taxi (m=1)

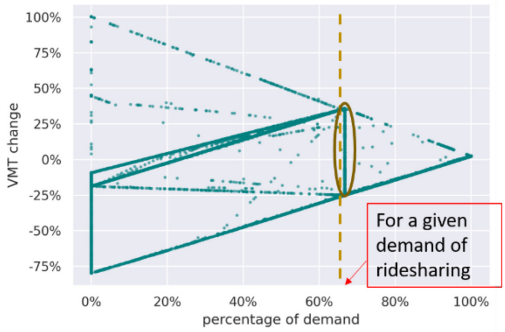

(b) Demand of ridesharing (m=2)

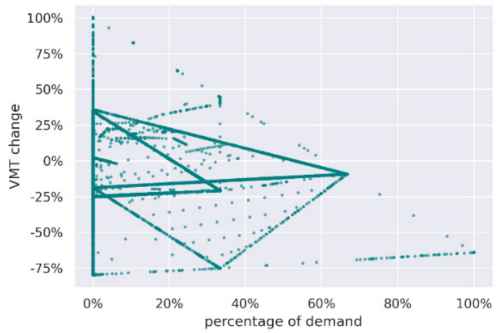

(c) Demand of Ttransit (m=3)

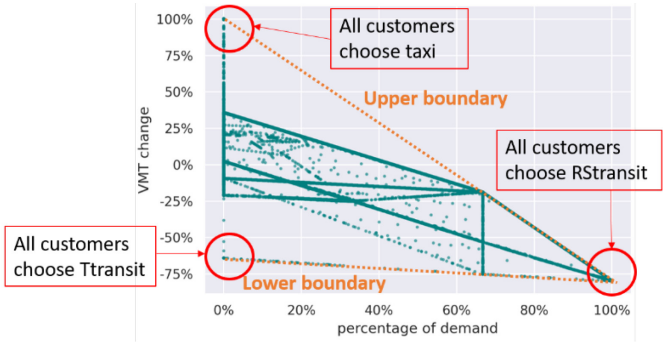

(d) Demand of RStransit (m=4)

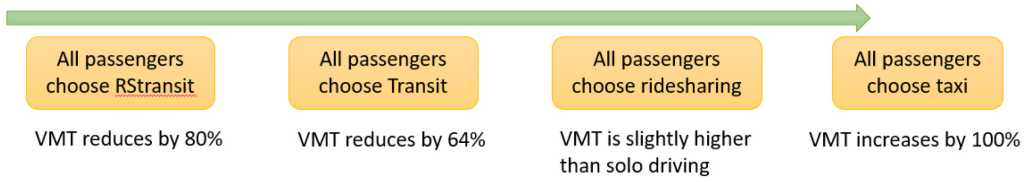

(e) Summary of corner cases

Figure 6 Demand versus VMT change

5.2 Numerical results of the Seattle U-District Network

In this numerical example, the University District (U-District) in Seattle was the residential area that generated the commute demand. Commuters from the U-District could commute to downtown Seattle for work by four modes, single/shared rides for the whole trip or the first mile (and then transfer to transit). We continued with the numerical experiment to analyze how commuters' mode choices changed with their value of time and the resulting congestion patterns. The numerical experiments on the Seattle network would provide more insights into the operation of the CAV integrated transit

system, as well as help with building next generation transportation demand management (TDM) strategies that will simultaneously increase the mobility of the city and relieve congestion.

5.2.1 Simplification of the Seattle U-District

The network provided by the Puget Sound Regional Council (PSRC, 2021) included 439 nodes and 1,241 links (Figure7). We simplified this network (combined nodes that were too close to each other, combined or eliminated very small links, etc.) so that it included only 150 nodes and 485 links, as shown in Figure 8. The simplified network consisted of two types of links: the original links (blue links in Figure 8) and new links (red links in Figure 8). The links that were cut into smaller sections were replaced with new links that directly connected the start node and the end node. For the morning commuting scenario, we assumed that all passengers (customers for the integrated transit system) traveled from the U-D-istrict to the downtown Seattle area. We chose the location of the Westlake Link station as the destination, as shown in Figure 9. We also assumed that each passenger chose one of the three routes from the U-District to the downtown area, and the three routes were simplified as three links (see the three links that connect the U-District with the downtown area in Figure 9). Link properties, such as length, free flow time, and capacity, were modified for the new links.

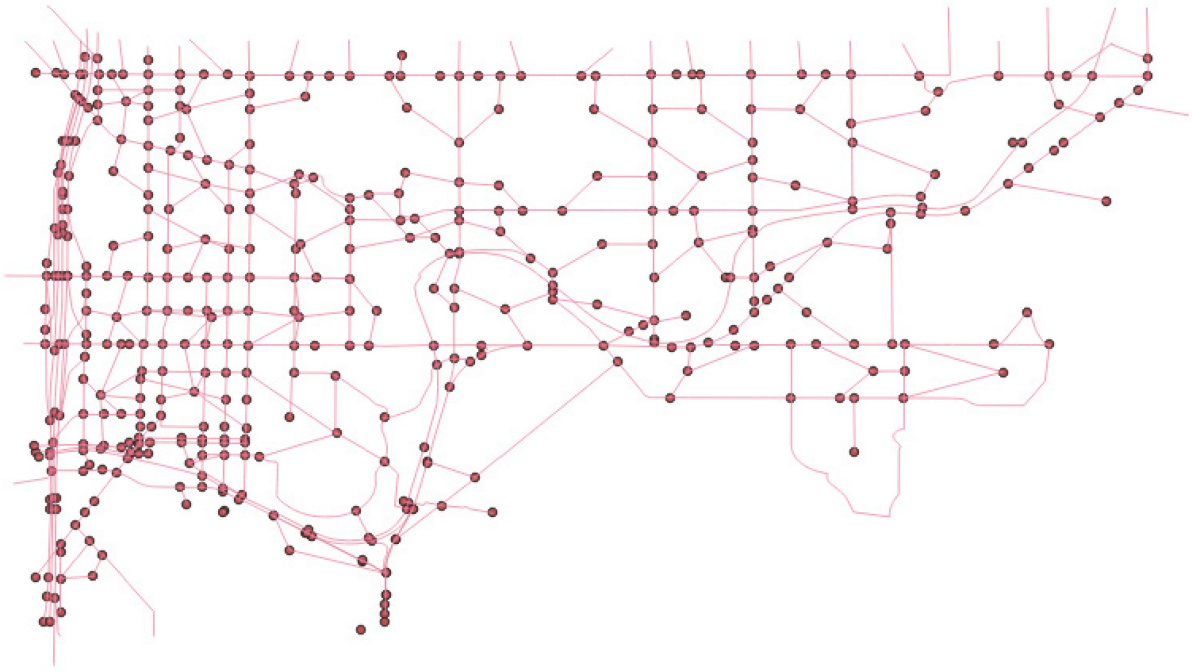

Figure 7 U-District: the original network (439 nodes, 1,241 links)

Figure 8 U-District: simplified network (150 nodes, 485 links)

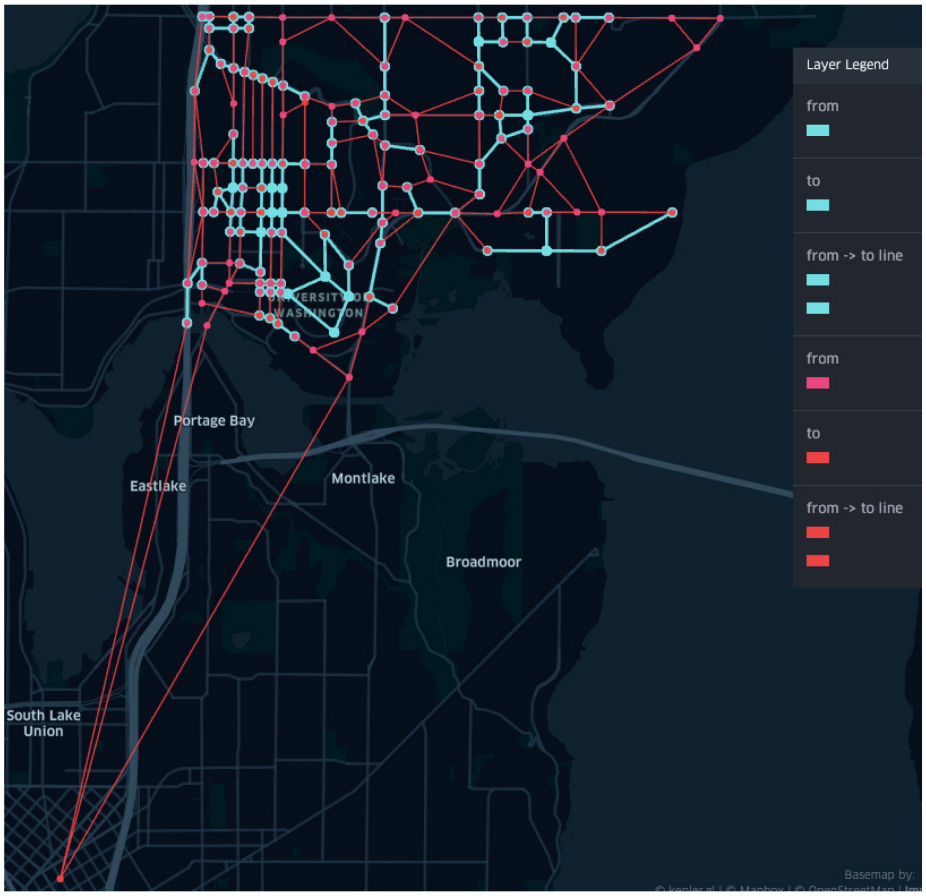

Figure 9 Hyperlinks to the downtown Seattle area

The demand from the U-District was aggregated at the traffic analysis zone (TAZ) level. Table 6 summarizes the labels of the TAZ we selected from the U-District and downtown areas. The U-District had 50 TAZs, and downtown had 137 TAZs. Figure 11 shows these TAZs in a map. For the U-District, we selected one node within each TAZ and set the node as an origin. The origin nodes are shown in Figure 10. The demand from the origin nodes to destination node 151 is shown in Table 7. We aggregated the demand for the 137 TAZs in the downtown area; as shown in Table 7, the demand from node 25 to node 151 was 218, meaning that the demand from TAZ 221 to the whole downtown area consisted of 218 people per hour.

Table 6 TAZs in the U-District and downtown

	The list of TAZs	The number of TAZs
U-District	201, 202, 203, 204, 205, 206, 207, 208, 209, 210, 211, 212, 213, 214, 215, 216, 217, 218, 219, 220, 221, 279, 280, 281, 282, 283, 284, 285, 286, 287, 288, 289, 290, 291, 292, 293, 294, 295, 296, 297, 298, 299, 300, 301, 302, 303, 304, 305, 306, 307, 308	50
Downtown	441, 438, 439, 437, 435, 433, 431, 429, 607, 616, 443, 444, 445, 446, 447, 448, 449, 450, 451, 452, 453, 454, 455, 456, 457, 458, 459, 460, 461, 462, 463, 464, 465, 466, 467, 468, 469, 470, 471, 472, 473, 474, 475, 476, 477, 478, 479, 480, 481, 482, 483, 484, 485, 486, 487, 488, 489, 490, 491, 492, 493, 494, 495, 496, 497, 498, 499, 500, 501, 502, 503, 504, 505, 506, 507, 508, 509, 510, 511, 512, 513, 514, 515, 516, 517, 518, 519, 520, 521, 522, 523, 524, 525, 526, 527, 528, 529, 530, 531, 532, 533, 534, 535, 536, 537, 538, 539, 540, 541, 542, 543, 544, 545, 546, 547, 548, 549, 550, 568, 569, 570, 571, 572, 573, 574, 575, 576, 577, 578, 579, 580, 581, 609, 610, 611, 612, 613	137

Figure 10 Origins

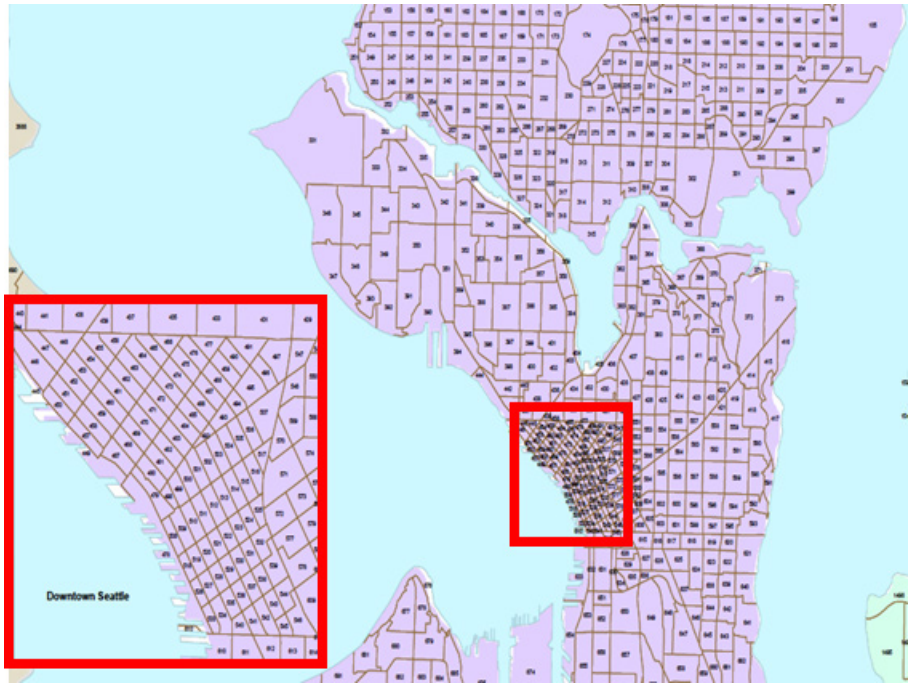

Figure 11 TAZs of the Seattle area (downtown Seattle is shown in the red box)

Table 7 Demand table for the Seattle network

origin -> destination	demand	origin -> destination	demand	origin -> destination	demand
25 -> 151	218	33 -> 151	195	83 -> 151	66
17 -> 151	224	18 -> 151	124	74 -> 151	124
15 -> 151	67	26 -> 151	125	58 -> 151	122
45 -> 151	89	55 -> 151	125	75 -> 151	279
13 -> 151	81	147 -> 151	235	103 -> 151	151
38 -> 151	90	47 -> 151	344	114 -> 151	76
11 -> 151	95	79 -> 151	475	113 -> 151	269
146 -> 151	63	59 -> 151	205	112 -> 151	95
10 -> 151	90	91 -> 151	152	150 -> 151	808
37 -> 151	125	57 -> 151	185	1 -> 151	0
9 -> 151	78	93 -> 151	100	142 -> 151	1546
40 -> 151	89	80 -> 151	68	107 -> 151	539
8 -> 151	103	49 -> 151	56	127 -> 151	36
43 -> 151	23	148 -> 151	252	134 -> 151	15
7 -> 151	69	50 -> 151	7	105 -> 151	508
39 -> 151	122	76 -> 151	63	133 -> 151	9
20 -> 151	206	149 -> 151	101		

5.2.2 Ridesharing Paris (RS Paris)

In the small network, because there were only three origin nodes, shared rides could happen between each pair of origins. For a large network, such as the Seattle network, it would be computationally expensive and practically uneconomical to allow shared rides between each pair of origin nodes. For example, if a shared ride vehicle first picked up a passenger at node 132 (shown at the lower left in Figure 10), it would not make sense for the platform to allow this vehicle to pick up the second passenger at node 16 (at the upper right in Figure 10) and then proceed to the destination in the downtown area. Note that our model chose from the top *k* shortest paths between each OD pair (origin-destination pair) and RS pair. If we had one path between each RS pair, then there would be 1*50*(50-1)=2,450 paths for RS pairs. With large numbers of paths, the running time of the MCP solver can be several hours, and it would be time consuming for us to conduct the sensitivity analysis. To reduce the computation time, we assumed that the distance between the two nodes in a RS pair was less than or equal to 1 mile, as shown in Figure 12. Under this assumption, there were 1,164 RS pairs in total. The

average number of RS pairs from a node was 23.28, which means after picking up the first passenger from an origin node, there were 23 among the other 49 nodes from which a shared-ride vehicle could choose to pick up the second passenger. Table 8 summarizes the statistics of the number of RS pairs from a node. The 25th percentile of the number of RS pairs that a node belonged to was 18, meaning that three-quarters of the nodes were the origins of more than 18 RS pairs.

Figure 12 Selecting two nodes within a 1-mile distance as RS pairs

Table 8 Statistics of the number of RS pairs from a node

mean	std	min	25%	50%	75%	max
23.28	7.761864	4	18	24	27.75	37

5.2.3 Cost Parameters

Table 9 lists the parameters of the U-District network. Table 9 reflects the following relationship between the fares of different modes: single ride > shared ride > transit, while customer disutility rates followed the relation single ride > shared ride. In the sensitivity analysis described later in this section, we modified some of these baseline parameters.

Table 9 Baseline parameters (Seattle network)

Illustration of parameters	Notation (m =1,2,3,4)	Value
The fixed fare for different modes ($)	F^m	6.8, 5.8, 6.8, 5.8
Time-based fare rate ($/h)	α_1^m	1.1, 0.5, 1.1, 0.5
Distance-based fare rate ($/mile)	α_2^m	1.5, 1.2, 1.5, 1.2
Conversion factor from time to cost ($/h)	β_1^m	3, 2.6, 3, 2.6
Conversion factor from distance to cost ($/mile)	β_2^m	1.2, 1.1, 1.2, 1.1
Value of time of customers, while traveling ($/h)	γ_1^m	3, 2.8, 3, 2.8
Value of time of customers, while waiting ($/h)	γ_2^m	3, 2.8, 3, 2.8
Value of time of customers, while mathing in shared rides ($)	γ_3^m (m=2,4)	NA, 1, NA, 1
Travel distance-based fare rate of transit ($/h)	α_3	0.5
Conversion factor from distance to cost for transit ($/mile)	γ_4	0.5
Transfer cost of transit ($/transfer)	γ_5	0.1

5.2.4 Results of Unilaterally Changing One Parameter

Table 10 shows the results when we unilaterally changed the travel distance-based fare rate of single rides. Under the current baseline parameter setting (Table 9), the demand for serving the whole trip using ridesharing ($m = 2$) was always zero, indicating that customers preferred the integrated modes or taxi over ridesharing. When taxi had a low travel distance-based fare rate ($\alpha_2^1 = 0.8$), the majority of customers (98.89 percent) chose taxi. When we unilaterally increased the distance-based fare rate of single rides ($\alpha_2^1 = \alpha_2^3$), the cost of requesting taxi increased, and more customer switched to request Ttransit; thus the demand for taxi decreased while the demand for Ttransit increased. When the distance-based fare rate of single rides ($\alpha_2^1 = \alpha_2^3$) continued to increase to 1.4, around 29 percent of customers switched from Ttransit to RStransit, since for some routes, taking RStransit cost less than Ttransit. This example shows that when the cost parameter for a taxi increased, customer choice of a taxi decreased, and the VMT of the entire network decreased. The VMT decreased because customers switched from the high VMT mode of taxi to the low VMT modes of Ttransit and RStransit.

Table 10 Unilaterally changing α_2^1

$\alpha_2^1 = \alpha_2^3$	Taxi, m=1	Ridesharing, m=2	Ttransit, m=3	RStransit, m=4	VMT (miles)
0.8	98.89%	0.00%	1.11%	0.00%	97402.20
0.9	32.36%	0.00%	67.64%	0.00%	46892.46
1.4	27.75%	0.00%	72.25%	0.00%	44019.52
1.5	27.36%	0.00%	43.29%	29.35%	38618.89
2	27.36%	0.00%	25.77%	46.87%	36500.68

5.2.5 Mode Choices vs. VMT Change

As in section 5.1.2, we compared the VMT of a certain mode split scenario to the case in which all customers drove alone in a personal vehicle. When all customers chose solo driving (no ridesourcing or transit involved), the VMT was equal to 49,414.34 vehicle miles based on the UE solution. Thus, the VMT change could be calculated as follows:

$$VMT\ change = \ (VMT\ of\ a\ particular\ scenario - 49414.34)/49414.34$$

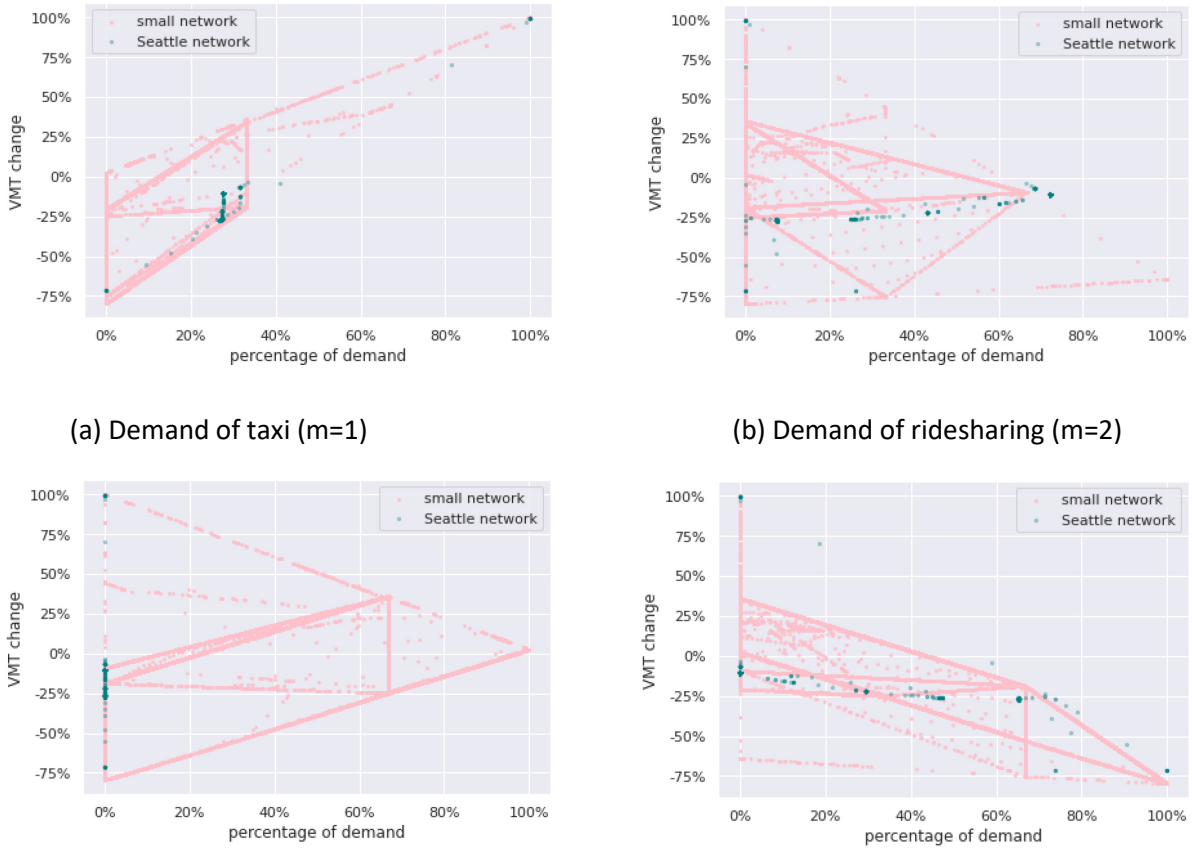

(a) Demand of taxi (m=1)

(b) Demand of ridesharing (m=2)

(c) Demand of Ttransit (m=3)

(d) Demand of RStransit (m=4)

Figure 13 Mode choices vs. VMT for the small network and the Seattle network

Figure 13 (a) – (d) shows the relationship between demand (expressed in terms of the percentage of total demand) for a particular mode $m \in \{1,2,3,4\}$ and VMT change. We plotted the results from the small network and the results from the Seattle network in the same graph. From Figure 13, we can see that the results from the Seattle network fell in the same triangular region as those of the small

network, indicating that our findings in the small network can be generalized to large-scale real networks.

6. Discussion

In the numerical experiments in section 5, we changed the parameters of the four modes, including the fixed fare, time-/distance-based fare, time-/distance-based disutility, customer waiting time cost, transfer cost, and matching cost. In reality, customers choose one mode over another based on multiple various factors. By setting different parameters, we can better reveal customers' mode choices. It is intuitive that when we increase the disutility parameters for some mode, fewer customers will choose that mode. Our results can capture this properly (tables 3, 4, 10). The proposed model can also capture more complex scenarios due to the interactions of different modes. For example, changing the parameters for transit caused the disutility of both Ttransit and RStransit to change. Changing the parameters for shared rides caused the disutility of both ridesharing and RStransit to change. This resembles the interactions of ridesourcing companies and transit agencies in practice. When a ridesourcing company changes the price of its shared-ride service, it may affect ridesharing and RStransit differently. Similarly, the disutility due to transit transfer may change when the transit company makes changes to its routes, stops, schedules, and fares. The increased transfer cost of taking transit may affect Ttransit and RStransit differently. Therefore, when there are changes to the parameters for transit and shared rides, the ways that customers exactly react to such changes can be quite complex, which can be captured by the model proposed in this study, as shown in figures 4 and 5.

On the other hand, different mode splits (resulting from customers' mode choices) may lead to varied VMT changes in comparison to all customers driving alone. Numerical experiments (Figure 6(e) in particular) showed that higher usage of transit or shared rides reduced VMT. Shared rides alone without transit (i.e., the ridesharing mode (m=2) used in this analysis) may still lead to slightly higher VMT in comparison to solo driving because of deadhead miles. The results thus clearly illustrated the important role of transit in serving commuters in urban areas. Although we only considered fixed route, fixed schedule mass transit (sometimes less efficient than on-demand transit) in this analysis, the numerical results showed that if all customers choose to use transit, the VMT reduction can be tremendous: 64 percent if the first mile is served by single rides (for Ttransit) or 80 percent if the first mile is served by shared-rides (for RStransit), as shown in Figure 6 (e). Furthermore, the numerical results in Section 4 were for a morning commute scenario in which travel demand was extremely asymmetric, i.e., all demand was from a common residential area to downtown worksites. This also explains why the VMT changes were large in general, from an 80 percent reduction (RStransit only) to a 100 percent increase (taxi only). For more symmetric demand patterns, we expect the VMT changes would be milder (see Ban et al., 2019). However, we believe that the general trend of the changes should be the same.

Our proposed model can thus help provide insights to transit agencies and ridesourcing companies for making sensible policies related to their operations and for potential collaboration on integrated ridesourcing and transit systems. The ability to capture network-wide congestion effects is also a

highlight of the model, since the evaluation of congestion levels in a multimodal network is important, especially if CAVs are widely deployed.

7. Conclusions

The era of CAVs may bring about a significant reduction in car ownership. This project envisioned a morning commuting scenario in which one ridesourcing platform operated all CAVs, providing single- or shared-ride services for commuters. CAVs would send customers either to their worksites or to transit hubs (major stations) to take transit to their worksites. This resulted in four modes for a customer to choose: taxi, ridesharing, Transit, and RStransit. We modeled the value of time/inconvenience of customers as an overall disutility by choosing a mode, encompassing various factors such as distance, waiting, matching, transfer, and the fare of the mode. At equilibrium, the ridesourcing company would maximize its profit, each customer would choose the mode with the lowest disutility, and the vehicular flow would be assigned to the network routes based on Wardrop's first principle, limiting network congestion. Analysis showed that the proposed model captures the behaviors and interactions of the ridesourcing platform and customers and can assess the congestion level of the network. This report also discusses insights into the modeling methods and results for integrating CAV-based ridesourcing services with fixed-route mass transit.

Future studies are recommended in the following areas:

- Test the proposed model on large, real-world networks. We tested the validity of our model by using a small network and then appling the model to the larger Seattle U-District network. Future studies could be conducted to apply the proposed model to the entire city of Seattle. The computation would be expensive for large, real-world networks. Scalability of the model would be the main challenge for such studies.
- Extend the current model to include other ridesourcing modes such as on-demand transit (i.e., micro-transit) and bikeshare services. In adding on-demand transit to the current model, the profit/efficiency of transit would need to be considered. In adding bikeshare services to the current model, the demand-supply balance of bikes in each zone would need to be considered. One possible way to do this would be to use the pricing strategy, i.e., set low prices for bike trips to zones that have low bike counts and high demand for bikes; and set high prices for bike trips to zones that have high bike counts and low demand for bikes
- Collaborate with ridesourcing companies to test the model by using large-scale, real-world trip data. Trip price data from ridesourcing companies could be used as the trip price parameters in our model. Human behavior data would also be useful. Currently, the customers' disutility function consists of major factors such as waiting/matching related costs or travel time/distance-based costs. Alternatively, customer disutility could be estimated by using human behavior data. The two methods could be compared to discuss the pros and cons of using data to estimate customer disutility.

- Test the model for more general scenarios. In this study we considered only morning commute scenarios. Our model could also test a network in which the demand was symmetric between each OD pair, e.g., for the Seattle network, there would be demand from the U-District to the downtown area, as well as demand from downtown to the U-District.

References

Ban, X.J., Dessouky, M., Pang, J.S. and Fan, R., 2019. A general equilibrium model for transportation systems with e-hailing services and flow congestion. Transportation Research Part B: Methodological, 129, pp.273-304.

Chen, P.W. and Nie, Y.M., 2017. Connecting e-hailing to mass transit platform: Analysis of relative spatial position. Transportation Research Part C: Emerging Technologies, 77, pp.444-461.

Di, X. and Ban, X.J., 2019. A unified equilibrium framework of new shared mobility systems. Transportation Research Part B: Methodological, 129, pp.50-78.

Feigon, S. and Murphy, C., 2016. Shared mobility and the transformation of public transit (No. Project J-11, Task 21).

Ke, J., Xiao, F., Yang, H. and Ye, J., 2019. Optimizing Online Matching for Ride-Sourcing Services with Multi-Agent Deep Reinforcement Learning. arXiv preprint arXiv:1902.06228.

Li, W., Cui. Z., Li, Y., Ban, X., 2019. Characterization of ridesplitting based on observed data: A case study of Chendu, China. Transportation Research Part C 100, 330-353.

Ma, T.Y., Rasulkhani, S., Chow, J.Y. and Klein, S., 2019. A dynamic ridesharing dispatch and idle vehicle repositioning strategy with integrated transit transfers. Transportation Research Part E: Logistics and Transportation Review, 128, pp.417-442.

Malucelli, F., Nonato, M. and Pallottino, S., 1999. Demand adaptive systems: some proposals on flexible transit. In Operational research in industry (pp. 157-182). Palgrave Macmillan, London.

Meyhofer, E., 2018. Uber and Toyota Team Up on Self-Driving Cars: Uber Newsroom US. [online] Uber Newsroom. Available at: <https://www.uber.com/newsroom/uber-toyota-team-self-driving-cars/> [Accessed 3 Dec. 2019].

Orski, C.K., 1976. Paratransit: The Coming of Age of a Transportation Concept. Transportation Research Board Special Report, (164).

Pinto, H.K., Hyland, M.F., Mahmassani, H.S. and Verbas, I.Ö., 2019. Joint design of multimodal transit networks and shared autonomous mobility fleets. Transportation Research Part C: Emerging Technologies.

PSRC, 2021. GIS Shapefiles. Puget Sound Regional Council (PSRC). Available at: https://www.psrc.org/gis-shapefiles [Accessed November 2, 2021].

Schaller Consulting, 2017. Unsustainable? The growth of app-based ride services and traffic. Travel and the Future of New York City (Accessed on April 20, 2018) http://schallerconsult.com/rideservices/unsustainable.htm .

Schaller Consulting, 2018. Estimating Uber and Lyft Ridership in the United States (Accessed on April 20, 2018) http://schallerconsult.com/rideservices/unsustainable.htm .

Shaheen, S., Chan, N., Bansal, A. and Cohen, A., 2015. Shared mobility: definitions, industry developments, and early understanding. University of California Berkeley Transportation Sustainability Research Center, Berkeley.

Stein, D.M., 1978. Scheduling dial-a-ride transportation systems. Transportation Science, 12(3), pp.232-249.

Terry, J. and Bachmann, C., 2020. Spatial characteristics of transit-integrated ridesourcing trips and their competitiveness with transit and walking alternatives. Transportation research record, 2674(3), pp.329-340.

Wardrop, J.G. and Whitehead, J.I., 1952. Correspondence. some theoretical aspects of road traffic research. Proceedings of the Institution of Civil Engineers, 1(5), pp.767-768.

Yan, X., Levine, J. and Zhao, X., 2019. Integrating ridesourcing services with public transit: An evaluation of traveler responses combining revealed and stated preference data. Transportation Research Part C: Emerging Technologies, 105, pp.683-696.